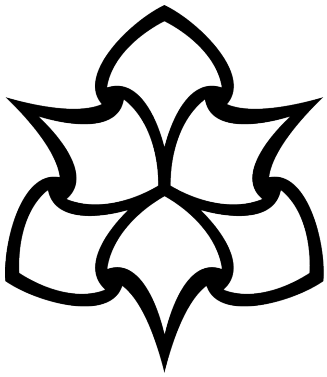

Informatics in Medicine Unlocked 12 (2018) 14–20

Contents lists available at ScienceDirect

Informatics in Medicine Unlocked

journal homepage: www.elsevier.com/locate/imu

The effect of filtering algorithms for breast ultrasound lesions segmentation

Fatima M. Osman [a,*], Moi Hoon Yap [b]

[a] Sudan University of Science and Technology, Khartoum, Sudan
[b] Manchester Metropolitan University, M1 5GD, UK

ARTICLE INFO

2017 MSC:
00-01
99-00

Keywords:
Ultrasound images
Jaccard similarity index
Filtering
Region-of-interest (ROI)
Breast lesion

ABSTRACT

Breast ultrasound images have a complicated structure, which is difficult to be segmented due to the fact that it has low signal and affected by noise ratio. Recent research concentrated on the Region of Interest (ROI) labeling and ROI segmentation. In order to reduce chances of human error, stages of processing in breast ultrasound images might be different from one another. This research proposes a new image filtering method for breast ultrasound, namely Altered Phase Preserving Dynamic Range Compression (APPDRC). In addition, this paper compares the performance of filtering algorithms, in combination with standard thresholding segmentation. Focusing on the filtering stage, a comparison between the proposed method APPDRC Filter and previous approaches is validated on a dataset of 306 images, namely Inverted Median filter, Multifractal Filter, Hybrid Filter, SRAD filter, and PPDRC. Further, a summary of the work to date on the effect of filtering on lesion segmentation in ultrasound breast images is reported. Jaccard Similarity Index (*JSI*) is used for evaluation, in which the automated segmentation result is compared with the experienced radiologist's manual delineation. Our results revealed that making the choice of filtering algorithm affects the final segmentation results. Considering Mean *JSI*, *Dice* and *MCC* metrics, the proposed APPDRC Filter achieved the best performance, and outperformed the five evaluated filtering methods.

1. Introduction

Due to the fact that early detection plays a main role in avoiding breast cancer deaths and increases the proportion of healing and recovery [1], a significant increase in early detection of cancer is noticed in the past few years [2–5]. For all women in the world, breast cancer is considered to be the second leading cause of death [6]. In Sudan, the real scope of cancer is not known, although the reported cases have increased from 303 (in 1967) to 6303 (in 2010) [7].

Initial lesion is the suspected region that is located manually by a specialized radiologist. It is determined by specifying the four boundaries (topmost, leftmost, bottommost and rightmost) by crosses, in a preprocessing stage [8,9]. Then, radiologist encompasses these four crosses to show the region of interest (ROI) within a rectangle, and present the preprocessed image to a computer-aided diagnosis system (CAD) for the segmentation and classification of the tumor [8]. Within the complex and irregular tissues of the breast, accurate detection and segmentation of suspicious regions, typically require human analysis and decision making [10]. Most radiologists find it uncomfortable trying to differentiate between solid masses in ultrasound images, which is caused by the large overlap in the sonographic appearance of malignant and benign lesions [11].

In order to decrease chances of human error, and get more accurate screening of cancer, the examiner should be well-trained and experienced with knowledge of breast anatomy, and the normal expected changes caused by pathology [12]. The performance of CAD system significantly depends on including an entire lesion within the ROI, or outlining ROIs that contain lesions in an input preprocessed image, which relies on humans experience that might vary from one radiologist to another [12].

In literature, significant interest has been shown in speckle reduction filters to filter BUS images, mainly because it is affected by speckle noise. Anisotropic diffusion algorithm was introduced by Perona and Malik in 1990 [13], and has been improved by many research works later [4,14–16].

On the other hand, regardless the formation of an image, monogenic filters were used in Ref. [17] to extract local phase and amplitude values across the image. This step is followed by a dynamic range reduction. Phase Preserving Dynamic Range Compression (PPDRC) method preserves the local phase information, and allows image reconstruction using the original phase values [17].

* Corresponding author.
E-mail addresses: fatma.m.osman@gmail.com (F.M. Osman), M.Yap@mmu.ac.uk (M.H. Yap).

https://doi.org/10.1016/j.imu.2018.04.008
Received 9 December 2017; Received in revised form 25 April 2018; Accepted 27 April 2018
Available online 8 May 2018

In this work we propose Altered Phase Preserving Dynamic Range Compression (APPDRC) filtering algorithm on breast ultrasound images, for further enhancement of PPDRC filter. Consequently, gray-scale inversion is applied on PPDRC filtered images, then Linear filter and Gaussian filter are applied subsequently. Additionally, the effect of APPDRC on BUS images is shown for the first time. Further, we present a review on the state-of-the-art breast ultrasound image filtering algorithms, namely: Inverted Median filter [18], Multifractal Filter [19], Hybrid Filter [20], SRAD Filter [4], PPDRC Filter [17], and the proposed APPDRC Filter. The performance of these filtering algorithms is compared on a standardized segmentation task, and results were validated on a breast ultrasound dataset with 306 ROIs. APPDRC method outperformed the five evaluated filtering algorithms in three evaluation metrics, i.e. *Jaccard Similarity Index (JSI), Dice Similarity Coefficient (Dice), and Mathew Correlation Coefficient (MCC)*.

In the Materials and Methods section, the proposed APPDRC Filter in BUS images is introduced, segmentation stage and performance measures metrics for evaluating the filtering algorithms are stated. In the Results section, APPDRC filter is tested on ROIs dataset, and its effect on segmentation stage is shown. Additionally, a comparison between the other five filtering methods is presented. In Discussion section, results of the study are discussed and comparison between filtering algorithms is reported. The final section is dedicated to the concluding remarks and future trends.

2. Related work

Ultrasound images are affected by some extent of noise. Noise is defined as unexplained variation in data disturbances in image intensity which are either uninterpretable or out of interest [21]. In order to simplify image analysis of breast ultrasound (BUS), many filtering algorithms were proposed. This section discusses the state-of-the-art pre--processing algorithms for BUS images.

In order to get an accurate segmentation, a typical preprocessing step in BUS images should be done, which is filtering stage (Denoising). Perona and Malik [13] proposed a non-linear and space invariant transformation of an image aiming at de-noising that image without removing significant parts of its content such as edges or lines. Based on a diffusion process, speckle reduction filter removes the noise by computing a local weighted average of the central pixel intensity with the ones of its neighbors. Anisotropic diffusion resembles the process that creates a scale space, in which a parameterized family of more blurred images is generated out of the image, and a convolution between the image and a 2D isotropic Gaussian filter is assigned to each image in the produced family [13].

In 2002 Yu and Acton [14], proposed Speckle Reducing Anisotropic Diffusion (SRAD) by improving the Anisotropic Diffusion method [13]. SRAD is an edge-sensitive diffusion for speckled images, it proposes a partial differential equation approach aiming to enhance edges in filtered images [14]. According to validation in Ref. [14], SRAD outperformed the traditional speckle removal filters and the conventional anisotropic diffusion method in terms of mean preservation, edge localization, and variance reduction.

In Ref. [18], radial gradient index (RGI) filtering is applied on a dataset of 757 images for 400 patients to detect lesions on breast ultrasound images. Then, they obtained segmentation by maximizing an average radial gradient (ARD). In their proposed scheme, 75% of the lesions were correctly detected at an overlap of 0.4 with a radiologist lesion outline. Using round robin analysis, they assessed the quality of the classification of lesion candidates into actual lesions and false positives by a Bayesian neural network. As a preprocessing step of RGI filtering, they applied a gray-scale inversion followed by median filtering. In this work, we consider the effect of this filtering step (Gray-scale Inverted Median Filter) in our evaluation.

A novel aspect was achieved by the use of a hybrid filtering in Ref. [20]. In order to produce edge-sensitive speckle reduction, a nonlinear diffusion was applied to images. Then edge smoothing step was applied on ultrasound images using linear filtering (Gaussian blur), which also eliminates oversegmentation. Followed by hybrid filtering, multifractals were used subsequently to further enhance the partially processed images [19]. In this work, both Multifractal Filter of [19], and Hybrid Filter of [20] are considered for evaluation.

In Ref. [22], they proposed Speckle Reducing Bilateral Filtering (SRBF), a fully automatic bilateral filter tailored to ultrasound images. Noise statistics were embedded in the filter framework to obtain edge preservation property. With respect to local statistics, their filter was able to tackle the multiplicative behavior modulating the smoothing strength. According to their results, SRBF filter showed a superior performance when compared with oriented anisotropic diffusion (OSRAD) filter of images.

In Ref. [4], they used speckle reducing anisotropic diffusion technique (SRAD) Filter [14]. In five steps, Shan et al. [4] proposed a novel and fully automated approach for BUS segmentation. Step 1: Speckle reduction using anisotropic diffusion (SRAD) [14]. Step 2: an automated threshold selection algorithm was proposed. Step 3: Connected components (possible lesion regions) were found by deleting boundary-connected regions. In which, a region was included in lesion candidate if list consists of the its boundary intersects with the center window (a window located at the image center, and about half size of the entire image). Further in step 4: Regions were ranked [4]. In Step 5: they determined the seed point, in order to get the most accurate ROI. The novel approach for fully automated lesion segmentation proposed in Ref. [4] included three major steps, first: an efficient region-of-interest (ROI) generation was applied, followed by multi-domain feature extraction using two newly proposed lesion features (namely: phase in max-energy orientation and radial distance), combined with a traditional intensity-and-texture feature. Third, lesions were detected by a trained artificial neural network. Within (ROI) generation, the first step was a method of automatic seed point selection, which was developed using Speckle Reducing anisotropic diffusion (SRAD) Filter [4,14]. We consider SRAD Filter in this work for evaluation.

For investigating the filtering effect on the whole process of lesions segmentation, Elawady et al. [23] proposed three stages approach, starting with the removal of speckle noise without affecting the important features of the image. For this filtering stage, three methods were investigated: Frost Filter, Detail Preserving Anisotropic Diffusion, and Probabilistic Patch-Based Filter. In second step, in order to provide an initial segmentation map, they tested each of these three filtering approaches with two segmentation algorithms: either Normalized Cut or Quick Shift. In addition to preprocessing and segmentation, their BUS images were postprocessed in a third step by selecting the correct region from a set of candidate regions, ground truth images were used for system evaluation, and according to their work, Frost Filter showed better system performance when combined with Quick Shift segmentation, and this combination is considered to be the best for real time applications among the investigated three combinations, due to its low computational cost [23]. Further, both of Detail Preserving Anisotropic Diffusion and Probabilistic Patch-Based filtering methods gave better performance in combination with Normalized Cut segmentation.

In spite of the fact that there are a lot of algorithms in the literature for filtering BUS images, all of these algorithms are tested in combination with different types of segmentation methods and different datasets. Hence, there are no available fair comparison to show which filtering method is better, and how those filtering methods affect the segmentation on BUS images. Therefore, in this research we focus on making a fair comparison between state-of-the-art image filtering algorithms, which is achieved by using a quite simple segmentation method and applying all filtering methods on a single dataset of 306 BUS images. Additionally, we proposed a new filtering algorithm that will be stated in next section.

3. Materials and methods

In order to investigate the effect of filtering algorithms on ROI segmentation, we used 306 ROI images as our dataset [24]. The dataset that has been investigated in this work was obtained from a professionally compiled compact disc (CD) of breast ultrasound images [35]. In 2001, this dataset was collected using (B&K Medical Panther 2002 and B&K Medical Hawk 2102), 8–12 MHz linear array transducer, with Average Image Size of 377 × 396 pixels. Expert radiologist processed each image manually, and marked the extreme points of the suspected lesions with crosses. Experiments in this study were performed using MATLAB R2015b.

In spite of the fact that automatic detection of ROIs is not meant to replace the radiologist labeling, it is meant to reduce the time that is consumed in labeling ROIs [4,20]. In addition, automated ROI labeling helps to indicate the existence of ROIs that might possibly be missed by radiologist. The approach introduced in Ref. [20] effectively supported the selection of ROI, and improved interpretation consistency. This approach have been evaluated by comparing its output with manual labeling of an expert radiologist. It showed an accuracy better than other three considered ROI labeling methods.

As in previous research [25,26], we implemented the filtering algorithms on the ROIs. Further, a comparison between six filtering algorithms is performed, i.e. (a) Inverted Median Filter of[18], (b) Multifractal Filter of [19], (c) Hybrid Filter of [20], (d) SRAD Filter of [4], (e) PPDRC Filter of [17], and (f) prposed APPDRC Filter. Further, simple Thresholding Segmentation is applied for fair comparison to show the effect of each filtering algorithm on the segmentation stage. Finally, the evaluation is been driven to investigate each filter using *Jaccard Similarity Index (JSI)* [18], *Dice Similarity Coefficient (Dice)* and *Matthew Correlation Coefficient (MCC)*. Fig. 1 shows a flowchart of the evaluation process for filtering algorithms.

3.1. Altered Phase Preserving Dynamic Range Compression algorithm (APPDRC)

3.1.1. PPDRC Filter

Ultrasound images (sonograms), are considered to be non-photographic images along with X-rays (radiography), and magnetic resonance imaging [27]. In Ref. [17], they proposed an algorithm that is applicable to a wide range of non-photographic scientific images. Taking no assumptions about the formation of feature types an image contains, or its range of values, this method preserves local features and also compresses the dynamic range of an image. Using monogenic filters, the method extracts local phase and amplitude values across the image. In order to reduce the dynamic range of the image, a range reducing function is applied to the amplitude values, such as logarithm, then the image is reconstructed using the original phase values [17]. The main advantage of this approach is that it outputs an image which retains the fidelity of its features within a greatly reduced dynamic range. Additionally, it has two more attributes; first, the local phase information is preserved, and second, high-pass filtering is used to control the scale of analysis by choosing the range of spatial frequencies for image reconstruction phase [17].

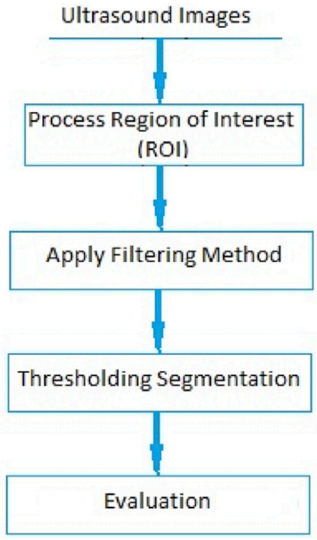

Fig. 1. An overview of the evaluation process for filtering algorithms.

Monogenic filters are used to obtain the local phase and amplitude, which are formed by combining a radial band-pass or high-pass filter with its Riesz transform. The Riesz transform forms a 2D equivalent of the Hilbert transform [36], each is made up of two filters in the 2D frequency domain (u_1, u_2) as shown in equation (1).

$$H_1 = i\frac{u_1}{\sqrt{u_1^2 + u_2^2}}, \quad H_2 = i\frac{u_2}{\sqrt{u_1^2 + u_2^2}} \tag{1}$$

The convolution kernel of the Riesz transform is defined by the spatial representation of the vector $H = (H_1, H_2)$. To obtain local phase and amplitude information the image, I, is convolved with the band-pass or high-pass filter f and the two Riesz transform filtered versions of f, $h_1 f$ and $h_2 f$ [17]. This provides three outputs, $I{*}f$, $I{*}h_1 f$ and $I{*}h_2 f$, where * denotes convolution. The local amplitude at image location (x, y) is given by:

$$A(x,y) = \sqrt{f(x,y)^2 + h_1 f(x,y)^2 + h_2 f(x,y)^2} \tag{2}$$

The local phase is given by

$$\phi(x,y) = atan2\left(f(x,y), \sqrt{h_1 f(x,y)^2 + h_2 f(x,y)^2}\right) \tag{3}$$

And orientation is given by

$$\theta(x,y) = \quad atan2(h_2 f(x,y), h_1 f(x,y)) \tag{4}$$

The reconstructed, tone mapped image values, $T(x, y)$ are given by

$$T(x,y) = \quad log(A(x,y) + 1).sin(\phi(x,y)) \tag{5}$$

According to [17], the use of high-pass filters is considered to be most useful, as it retains all the high frequency components of the signal in order to preserve fine details of the image. In this work, dynamic range compression algorithm is applied with high-pass cutoff frequency of 1/10000, and cutoff spatial frequency of 220 pixels.

3.1.2. APPDRC

According to the output of previous stage, PPDRC filter reduces the contrast and intensity variations of the image, which enables a better intensity-based segmentation by thresholding. In a complementary step, for further enhancing the partially processed ROIs, the need to enhance filtering of speckle noise is essential for better boundary detection. Accordingly, a gray-scale inversion followed by a combination of Linear Filter and Gaussian Filter is applied on the PPDRC filtered images. This proposed approach is referred to as Altered Phase Preserving Dynamic Range Compression (APPDRC).

After applying the two steps of filtering, a Completely Automated Threshold Segmentation approach is used for fair comparison with other filtering algorithms.

3.2. Segmentation

As this work focuses on filtering algorithms, a Completely Automated Threshold Segmentation approach is used because of its simplicity. In order to compare and validate the results of different filtering algorithms on BUS images, we assess its effect on the segmentation results. For fair

comparison, the segmentation stage uses Standard Thresholding algorithm [28].

The result of this approach will be visually compared with the results of other filtering algorithms. Using threshold segmentation approach [28], in which a parameter θ, called the brightness threshold is chosen and applied to the image a[m,n], as shown by equation (6).

$$\begin{array}{lll} & & IF \quad a[m,n] > \theta \\ Then & a[m,n] := 1 & (Object) \\ else & a[m,n] := 0 & (Background) \end{array} \tag{6}$$

3.3. Performance measures

In order to show the effect of filtering algorithms, usually performances indexes are used to report noise reduction. But, due to the fact that ground truth of the clean images is not available, *Jaccard Similarity Index (JSI)* is used to support evaluation of noise reduction metrics. Hence, by applying simple Thresholding segmentation the effect of each filtering algorithm on segmentation stage is assessed.

Accordingly, the first performance metric that we used for our work by using overlap, would be similar to the "overlap" figure used in Ref. [18]. *JSI*, which is defined as the ratio of intersection and union of the two lesion areas that were manually identified by the radiologist and by the computer-based algorithm. Using *JSI*, the overlap would be applied in images that consist of BUS lesions. As in Ref. [18], the design goal has been to achieve an overlap value in excess of 0.4, which is shown by equation (7):

$$Overlap = \frac{X \cap Y}{X \cup Y} \geq \quad 0.4 \tag{7}$$

where X is the lesion area extracted by the computer-based algorithm, and Y is the lesion labeled manually by the radiologist.

In addition to *JSI*, the results of the segmentation will be compared visually. Fig. 2 shows the overlapping between the automatically segmented image and the manual segmentation of radiologist. As per the fact that segmentation is considered to be successful when *JSI* is greater than or equal to 0.4 [18], the *JSI* value of Fig. 2 ROI image is 0.7827.

The other two commonly used evaluation metrics for performance of segmentation in medical imaging research are: *Dice Similarity Coefficient (Dice),* and *Matthew Correlation Coefficient (MCC)* [29]. If TP represents the number of true positives, TN true negatives, FP false positives, and FN false negatives, then *Dice* and *MCC* are defined as:

$$Dice = \frac{2*TP}{(2*TP + FP + FN)} \tag{8}$$

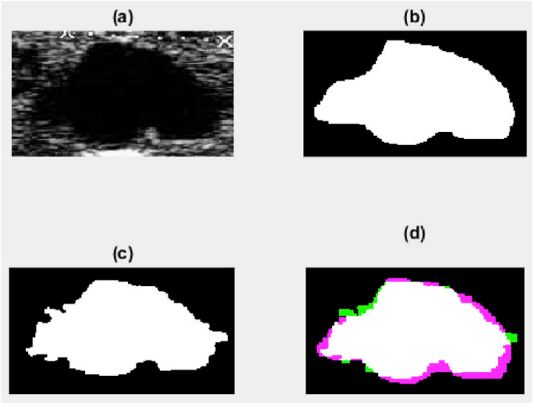

Fig. 2. Overlapping ROIs for (a) Original image, (b) Manual delineation by radiologist, (c) Automated segmentation of (APPDRC), and (d) Overlap between b and c.

$$MCC = \frac{TP*TN - FP*FN}{\sqrt{(TP + FP)(TP + FN)(TN + FP)(TN + FN)}} \tag{9}$$

4. Results

In order to evaluate filtering algorithms, a simple Thresholding Segmentation was applied, and then *JSI* for computer segmentation, and manual delineation by experienced radiologist was calculated.

Fig. 3 shows an original ROI, and a comparison of six filtering algorithms, namely; Inverted Median Filter [18], Multifractal Filter [19], Hybrid Filter [20], SRAD Filter [4], PPDRC Filter [17], and APPDRC Filter.

Fig. 4 visually compares the effect of the six investigated filtering algorithms on segmentation stage. We observed that APPDRC outperformed PPDRC and achieved comparable results to Multifractal Filter and SRAD Filter. A comparison of segmentations between PPDRC Filter [17] and the proposed APPDRC Filter is shown in Fig. 5.

Fig. 6 compares between *JSI* values achieved by each of the six filtering algorithm in five ranges within ($0.0 <= JSI <= 1.0$), showing the number of images successfully detected with *JSI* value of specific range. Fig. 7 shows a comparison between *JSI* values achieved in the proposed APPDRC Filter and the PPDRC Filter.

Table 1 summarizes the evaluation of filtering algorithms in three evaluation metrics, namely, *JSI*, *Dice*, and *MCC*. According to the results, the mean *JSI* of Multifractal Filter was 0.6258, 0.7181 for Hybrid Filter, 0.6715 for PPDRC Filter, 0.7141 for Inverted Median Filter, and 0.7094 for SRAD Filter. The results revealed that our proposed APPDRC Filter outperformed the five evaluated filtering methods with mean *JSI* of 0.7509. In addition to the best mean *JSI*, proposed APPDRC Filter achieved the best results with *Dice* score of 0.8685 ± 0.0666 and *MCC* score of 0.8662 ± 0.0662.

5. Discussion

In this article, APPDRC Filter for BUS images is proposed. After reducing the contrast and intensity variations of ROIs, speckle noise is successively reduced by applying gray-scale inversion followed by a combination of Linear filtering and Gaussian Filter. Moreover, simple thresholding segmentation is used for fair comparison with other state-of-the-art filtering algorithms.

Most of the commonly used measures for evaluation of filtering algorithms require the availability of the original image and the reconstructed image from its degraded version for reporting noise reduction, such as mean square error (MSE), root mean square error (RMSE) [30], signal-to-noise ratio (SNR), peak signal-to-noise ratio (PSNR) [31], and mean structure similarity index map (MSSIM) [32]. Due to unavailability of clean ground truth of images, a unique method of evaluation for filtering algorithms is assessed by applying simple thresholding segmentation on each filter. Thus, the evaluation of the segmentation is referred to the corresponding filter. We believe that unifying the segmentation and making it much simple, gives a quite fair comparison between filtering algorithms.

Fig. 3 compares the effects of using the six investigated filtering techniques. As noticed, the Median filter of (b) is inverted [18]. Hence, to achieve accurate evaluation, one exception is made by getting ROI's complement of the Inverted Median filtered ROI before heading to segmentation stage. As illustrated in (e), the SRAD Filter of [4] is relatively giving the highest smoothing effect when compared to other filtering methods, but it also shows the lowest speckle noise, giving a more clear lesion/non-lesion vision. In addition, when Multifractal Filter of [19] shown in (c) is used, high brightness is noticed around lesions, which causes a problem as it affects edge detection and lesion segmentation.

In Fig. 4, it is quite clear that PPDRC Filter of [17] is giving high noise on the segmentation stage, which leads to the fact that this approach should be used as a partial step in preprocessing stage for better

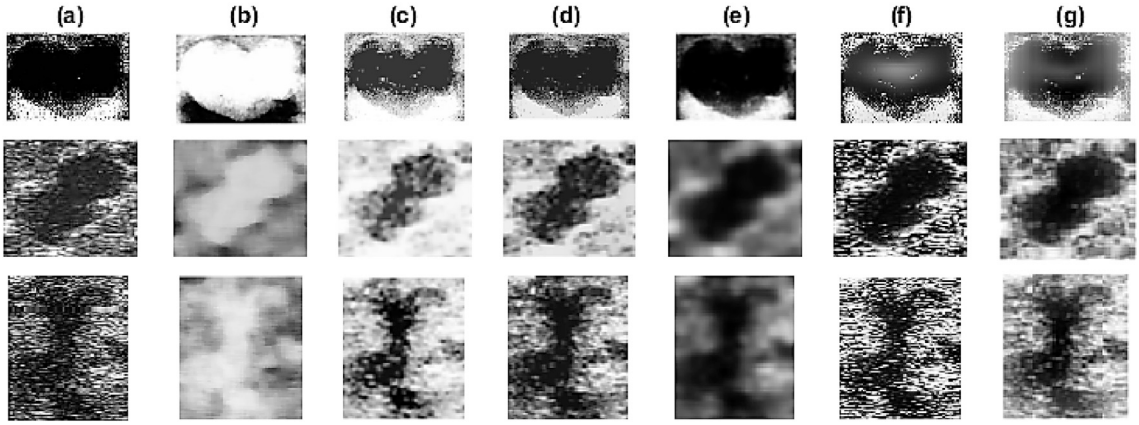

Fig. 3. Comparison of filtering algorithms for (a) original ROI, (b) Inverted Median Filter [18], (c) Multifractal Filter [19], (d) Hybrid Filter [20], (e) SRAD Filter [4], (f) PPDRC Filter [17], and (g) Proposed APPDRC Filter.

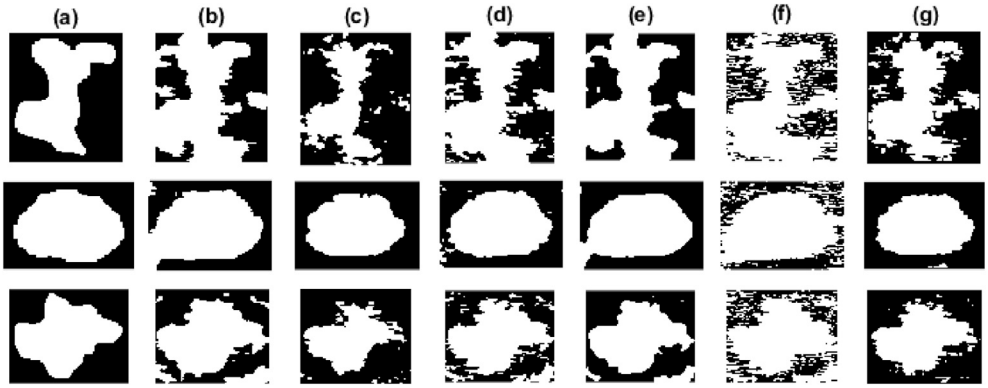

Fig. 4. Comparison of segmentation using (a) Ground Truth (Manual delineation), (b) Inverted Median Filter [18], (c) Multifractal Filter [19], (d) Hybrid Filter [20], (e) SRAD Filter [4], (f) PPDRC Filter [17], and (g) Proposed APPDRC Filter.

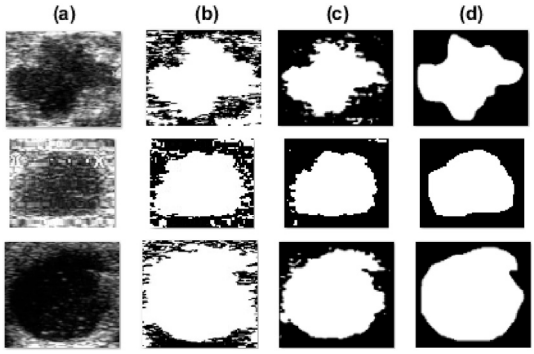

Fig. 5. Comparison of segmentation using (a) Original ROI, (b) PPDRC Filter [17], (c) Proposed APPDRC Filter, and (d) Ground Truth (Manual delineation).

segmentation on BUS images, and not to be taken alone. Although it was concluded in Ref. [19] that using Multifractal Filter enhances edge detection, we noticed that applying Multifractal Filter of [19] shows an oversegmentation of lesions. This is due to the high brightness noticed around lesions in the filtered ROIs of Fig. 3 (c), which affects negatively the lesion's edges when segmented using Thresholding segmentation.

As could be clearly noticed in Fig. 5, PPDRC Filter provides intensity-based segmentation by reducing contrast and intensity variations of images. Although, speckle noise around lesions still needs to be removed, which was achieved by the complementary filtering in the proposed APPDRC Filter, in which a combination of gray-scale inversion followed by a Linear Filter and Gaussian Filter is applied.

As shown in Fig. 6, all filtering algorithms provided better performance with ($0.6 <= JSI <= 0.8$), with more than (240 out of 306) images were provided by PPDRC Filter, however Multifractal Filter provided this range of *JSI* values for only (151 out of 306) images. Proposed APPDRC Filter showed the best performance in which (109 out of 306) images were successfully segmented with ($0.8 <= JSI <= 1$).

Fig. 7 illustrates the enhancement achieved in the proposed APPDRC Filter over the PPDRC Filter. In comparison with PPDRC filtering, lower number of images were provided by APPDRC Filter in the scale of ($0.6 <= JSI <= 0.8$). This is due to the fact that APPDRC Filter provided higher number of successfully segmented images (109 out of 306) in the scale of ($0.8 <= JSI <= 1$). In similar study [22], *JSI* scores were used to compare between two filtering algorithms, namely, Speckle Reducing Bilateral Filtering (SRBF) and Oriented Speckle Reduction Anisotropic Diffusion (OSRAD) [22].

6. Concluding remarks and future trends

This paper proposed APPDRC Filter and studied the effect of filtering algorithms on breast ultrasound lesions segmentation. Our results revealed that differences between the six filtering algorithms considered in this research are not huge. However, it shows that choosing the filtering algorithm affects the final segmentation results. Proposed APPDRC Filter achieved the best performance compared to other filtering algorithms evaluated, with *Dice* score of 0.8685 ± 0.0666 and *MCC* score

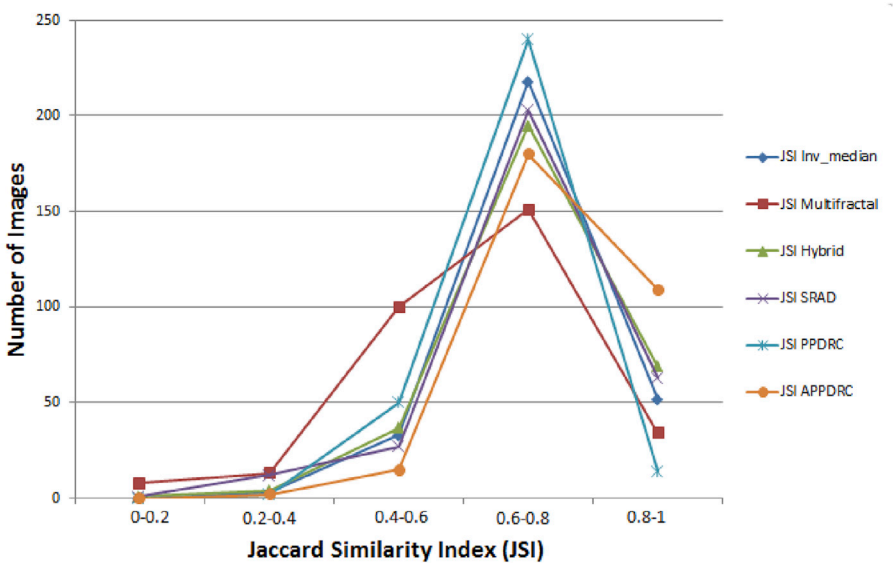

Fig. 6. Comparison of *JSI* values for: Inverted Median Filter of [18], Multifractal Filter of [19], Hybrid Filter of [20], SRAD Filter of [4], PPDRC Filter of [17], and proposed APPDRC Filter.

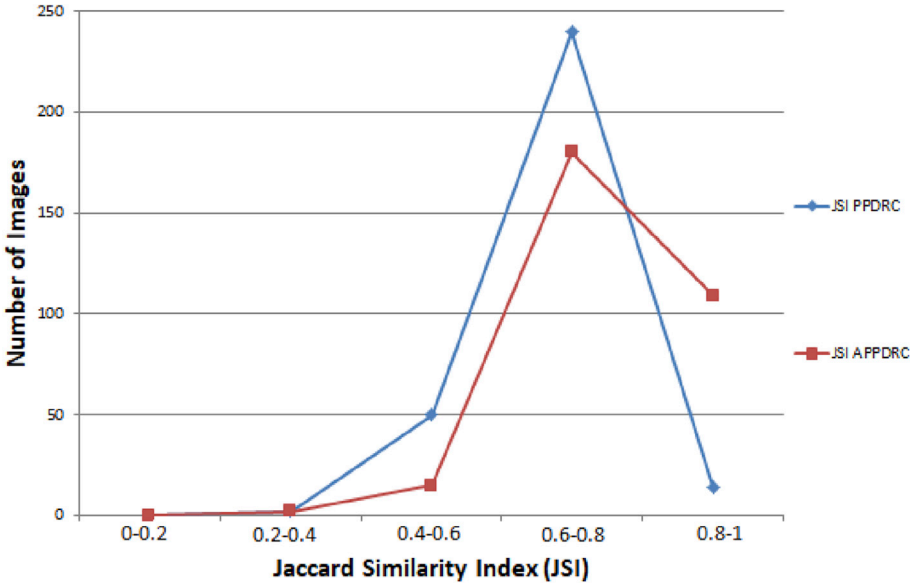

Fig. 7. Comparison of *JSI* values for: PPDRC Filter of [17], and proposed APPDRC Filter.

Table 1
Performance Measures for Various Filtering Algorithms. Bold indicates best results.

Authors, year, Ref	Algorithm	JSI	Dice	MCC
Drukker et al., 2002 [18]	Inv-Median	0.7141±0.0981	0.8461±0.0671	0.8427±0.0616
Yap et al., 2006 [19]	Multifractal	0.6258±0.1530	0.7874±0.1310	0.7861±0.1217
Yap et al., 2008 [20]	Hybrid	0.7181±0.1100	0.8513±0.0839	0.8429±0.0842
Kovesi et al., 2012 [17]	PPDRC	0.6715±0.0928	0.8087± 0.0708	0.8072±0.0620
Shan et al., 2012 [4]	SRAD	0.7094±0.1220	0.8503±0.0950	0.8438±0.0942
Proposed method	APPDRC	0.7509 ± 0.0929	0.8685 ± 0.0666	0.8662 ± 0.0662

of 0.8662±0.0662. In addition, proposed APPDRC Filter achieved best performance with highest number of images (109 out of 306) successfully segmented with score of (0.8 <= *JSI* <= 1). Our results also revealed that the proposed APPDRC achieved best average mean *JSI* of 0.7509, when compared with other filtering methods. Future work will investigate the potential of this filtering algorithms for data augmentation to improve recent works in deep learning [33,34]. Additionally, expanding the scope of compared filtering methods, by considering additional speckle reduction filters, like Speckle Reducing Bilateral Filtering (SRBF), and Oriented Speckle Reduction Anisotropic Diffusion (OSRAD) of [22], would increase the value of the filtering evaluation method proposed.

Conflict of interest

None declared.

References

[1] Cheng H, Shi X, Min R, Hu L, Cai X, Du H. Approaches for automated detection and classification of masses in mammograms. Pattern Recogn 2006;39(4):646–68.
[2] Yap MH, Edirisinghe EA, Bez HE. Fully automatic lesion boundary detection in ultrasound breast images. In: Medical imaging, international society for optics and photonics; 2007. 65123I–65123I.
[3] Yap MH, Edirisinghe E, Bez H. Processed images in human perception: a case study in ultrasound breast imaging. Eur J Radiol 2010;73(3):682–7.
[4] Shan J, Cheng H, Wang Y. Completely automated segmentation approach for breast ultrasound images using multiple-domain features. Ultrasound Med Biol 2012; 38(2):262–75.
[5] Deshmukh J, Bhosle U. Glcm based improved mammogram classification using associative classifier. Int J Image Graph Signal Process 2017;9(7).
[6] Cheng H, Shan J, Ju W, Guo Y, Zhang L. Automated breast cancer detection and classification using ultrasound images: a survey. Pattern Recogn 2010;43(1): 299–317.
[7] A. Elamin, M.E. Ibrahim, D. Abuidris, Cancer in sudanburden, distribution, and trends breast, gynecological, and prostate cancers.
[8] Chen D-R, Chang R-F, Chen W-M, Moon W-K. Computer-aided diagnosis for 3-dimensional breast ultrasonography. Arch Surg 2003;138(3):296–302.
[9] Gómez-Flores W, Ruiz-Ortega BA. New fully automated method for segmentation of breast lesions on ultrasound based on texture analysis. Ultrasound Med Biol 2016; 42(7):1637–50.
[10] Mogatadakala KV, Donohue KD, Piccoli CW, Forsberg F. Detection of breast lesion regions in ultrasound images using wavelets and order statistics. Med Phys 2006; 33(4):840–9.
[11] Horsch K, Giger ML, Venta LA, Vyborny CJ. Automatic segmentation of breast lesions on ultrasound. Med Phys 2001;28(8):1652–9.
[12] Chen D-R, Chang R-F, Huang Y-L. Breast cancer diagnosis using self-organizing map for sonography. Ultrasound Med Biol 2000;26(3):405–11.
[13] Perona P, Malik J. Scale-space and edge detection using anisotropic diffusion. IEEE Trans Pattern Anal Mach Intell 1990;12(7):629–39.
[14] Yu Y, Acton ST. Speckle reducing anisotropic diffusion. IEEE Trans Image Process 2002;11(11):1260–70.
[15] Krissian K, Westin C-F, Kikinis R, Vosburgh KG. Oriented speckle reducing anisotropic diffusion. IEEE Trans Image Process 2007;16(5):1412–24.
[16] Choi H, Jeong J. Despeckling images using a preprocessing filter and discrete wavelet transform-based noise reduction techniques. IEEE Sensor J 2018;18(8): 3131–9.
[17] Kovesi P. Phase preserving tone mapping of non-photographic high dynamic range images. In: Digital image computing techniques and applications (DICTA), 2012 international conference on. IEEE; 2012. p. 1–8.
[18] Drukker K, Giger ML, Horsch K, Kupinski MA, Vyborny CJ, Mendelson EB. Computerized lesion detection on breast ultrasound. Med Phys 2002;29(7): 1438–46.
[19] Yap MH, Edirisinghe EA, Bez HE. Object boundary detection in ultrasound images. In: Computer and robot vision, 2006. The 3rd canadian conference on. IEEE; 2006. 53–53.
[20] Yap MH. A novel algorithm for initial lesion detection in ultrasound breast images. J Appl Clin Med Phys 2008;9(4).
[21] Dogra A, Bhalla P. Image sharpening by Gaussian and butterworth high pass filter. Int J Adv Biol Biomed Res 2015;3(1):93–6.
[22] Balocco S, Gatta C, Pujol O, Mauri J, Radeva P. Srbf: speckle reducing bilateral filtering. Ultrasound Med Biol 2010;36(8):1353–63.
[23] Elawady M, Sadek I, Shabayek AER, Pons G, Ganau S. Automatic nonlinear filtering and segmentation for breast ultrasound images. In: International conference image analysis and recognition. Springer; 2016. p. 206–13.
[24] Yap MH, Pons G, Martí J, Ganau S, Sentís M, Zwiggelaar R, Davison AK, Martí R. Automated breast ultrasound lesions detection using convolutional neural networks. IEEE J Biomed Health Inform 2018:1. https://doi.org/10.1109/JBHI.2017.2731873. ISSN: 2168-2194, https://ieeexplore.ieee.org/abstract/document/8003418/.
[25] Huang Q, Luo Y, Zhang Q. Breast ultrasound image segmentation: a survey. Int J Comp Assist Radiol Surg 2017:1–15.
[26] Yap MH, Ewe H. Region of interest (roi) detection in ultrasound breast images. In: Proceedings of MMU international symposium on information and communications technologies (M2USIC); 2005. p. 5–8.
[27] Wells L. Photography: a critical introduction. Routledge; 2015.
[28] Sahoo PK, Soltani S, Wong AK. A survey of thresholding techniques. Comput Vis Graph Image Process 1988;41(2):233–60.
[29] D.M. Powers, Evaluation: from precision, recall and f-measure to roc, informedness, markedness and correlation.
[30] Willmott CJ, Matsuura K. Advantages of the mean absolute error (mae) over the root mean square error (rmse) in assessing average model performance. Clim Res 2005;30(1):79–82.
[31] Damera-Venkata N, Kite TD, Geisler WS, Evans BL, Bovik AC. Image quality assessment based on a degradation model. IEEE Trans Image Process 2000;9(4): 636–50.
[32] Wang Z, Bovik AC, Sheikh HR, Simoncelli EP. Image quality assessment: from error visibility to structural similarity. IEEE Trans Image Process 2004;13(4):600–12.
[33] Huynh B, Drukker K, Giger M. Mo-de-207b-06: computer-aided diagnosis of breast ultrasound images using transfer learning from deep convolutional neural networks. Med Phys 2016;43(6). 3705–3705.
[34] Yap MH, Goyal M, Osman F, Ahmad E, Martí R, Denton E, Juette A, Zwiggelaar R. End-to-end breast ultrasound lesions recognition with a deep learning approach. Med Imaging 2018: Biomed Appl Mol Struct Funct Imag 2018;10578. pages 1057819, International Society for Optics and Photonics.
[35] Prapavesis S, Fornage B, Palko A, Weismann C, Zoumpoulis P. Breast Ultrasound and US-Guided Interventional Techniques: A Multimedia Teaching File. Greece: Thessaloniki; 2003.
[36] Felsberg M, Sommer G. A new extension of linear signal processing for estimating local properties and detecting features, Mustererkennung 2000. Springer; 2000. p. 195–202.